


Spencer, T. C., J. B. Fallon, P. C. Thien, and M. N. Shivdasani. 2016. Spatial Restriction of Neural Activation Using Focused Multipolar Stimulation With a Retinal Prosthesis. *Investigative Ophthalmology & Visual Science*. **57**: 3181-91.

# Spatial Restriction of Neural Activation Using Focused Multipolar Stimulation With a Retinal Prosthesis

Thomas C. Spencer,[1,2] James B. Fallon,[1,2] Patrick C. Thien,[1,2] and Mohit N. Shivdasani[1,2]

[1]Bionics Institute, East Melbourne, Australia
[2]Department of Medical Bionics, The University of Melbourne, East Melbourne, Australia

Correspondence: Mohit N. Shivdasani, Bionics Institute, 384-388 Albert Street, East Melbourne, VIC 3002, Australia; mshivdasani@bionicsinstitute.org.

Submitted: February 11, 2016
Accepted: May 20, 2016

Citation: Spencer TC, Fallon JB, Thien PC, Shivdasani MN. Spatial restriction of neural activation using focused multipolar stimulation with a retinal prosthesis. *Invest Ophthalmol Vis Sci*. 2016;57:3181–3191. DOI:10.1167/iovs.16-19325

**Purpose.** The resolution provided by present state-of-the-art retinal prostheses is severely limiting for recipients, partly due to the broad spread of activation in the retina in response to monopolar (MP) electrical stimulation. Focused multipolar (FMP) stimulation has been shown to restrict neural activation in the cochlea compared to MP stimulation. We extended the FMP stimulation technique to a two-dimensional electrode array and compared its efficacy to MP and hexapolar (HP) stimulation in the retina.

**Methods.** Normally-sighted cats ($n = 6$) were implanted with a suprachoroidal electrode array containing 42 electrodes. Multichannel multiunit spiking activity was recorded from the visual cortex in response to MP, HP, and FMP retinal stimulation.

**Results.** When inferring retinal spread using voltage recordings off the stimulating array, FMP stimulation showed significantly reduced voltages in regions surrounding the primary stimulating electrode. When measuring the retinal and cortical selectivity of neural responses, FMP and HP stimulation showed significantly higher selectivity compared to MP stimulation (separate 2-way ANOVAs, $P < 0.05$). However, the lowest cortical thresholds for each stimulating electrode were higher for FMP and HP compared to MP stimulation (1-way ANOVA, $P < 0.001$). No significant differences were observed between FMP and HP stimulation in any measures.

**Conclusions.** Focused multipolar and HP stimulation using a two-dimensional array are promising techniques to reduce the spread of activation for a retinal prosthesis. Clinical application would be expected to result in smaller phosphenes; thus, reducing phosphene overlap between electrodes and increasing the resolution at the expense of higher thresholds for activation.

Keywords: retinal prosthesis, electrical stimulation, current focusing, in vivo electrophysiology, suprachoroidal

Retinitis pigmentosa (RP) is one of the most common forms of visual impairment, with over one million people affected worldwide.[1] It is characterized by a progressive loss of photoreceptors in the retina[1] resulting in the majority of RP sufferers becoming legally blind by the age of 40. No treatment currently is available to halt or reverse the degenerative effects.[1] As a result, prosthetic devices have emerged as a way to restore function by providing artificial input to the visual system.[2–6] These devices work by electrically stimulating residual neurons in the visual pathway.[6] The retina has become a favored region for prosthetic intervention due to a well-understood topographic map of visual space,[7] its early placement in the visual processing pathway, the relative ease of surgical access, and reasonable preservation of nonphotoreceptor neural circuitry.[8,9] When individual electrodes on a retinal prosthesis are stimulated, patients are able to perceive discrete flashes of light.[10,11] These flashes, termed phosphenes, are used as building blocks to generate an artificial image, much like pixels on a computer monitor. A number of groups have undertaken human clinical trials that use either the epiretinal,[3,12,13] subretinal,[14–17] or suprachoroidal[2,4] locations for implantation of electrode arrays.

The two commercially available devices, Second Sight's (Sylmar, CA, USA) Argus II and Retina Implant AG's (Reutlingen, Germany) Alpha IMS, use epiretinal and subretinal placements, respectively. However, suprachoroidal placement has the advantage of a relatively noninvasive implantation procedure,[18,19] albeit with higher levels of stimulation required to reach activation thresholds.[4,20,21] Higher stimulation levels have a detrimental effect on charge containment, impeding the formation of discrete phosphenes and limiting the visual resolution afforded to the patient. Being able to discriminate between phosphenes is an important factor in comprehending the image presented, which may not be possible using conventional methods of stimulation.[5,22] Another factor that may limit resolution is the interactions between overlapping electric fields generated by simultaneous stimulation of electrodes.[23,24] Channel interaction can result in activation of neural regions outside of the individual range of each electrode due to the effects of the summed current fields. This is an established phenomenon in cochlear[25–27] and retinal implants,[23,24,28–30] resulting in unpredictable spectral or spatial smearing of the percept. While this typically is circumvented using sequential stimulation presented within the flicker fusion rate of the visual system (~50 Hz), spatiotemporal interactions

between neural populations will become more prominent as timing is compressed to accommodate for an increasing number of stimulating electrodes.[24,30]

Current focusing techniques have been suggested to restrict the spread of current with the aim of reducing channel interactions and producing more discrete phosphenes.[23,31,32] Cochlear implant studies show that the electrode return mode used during stimulation, such as bipolar and tripolar (TP) stimulation, can significantly reduce the spread of neural activation in the cochlea and also can reduce the extent of auditory brain activation.[33–37] Similar approaches have been attempted in the retina, such as the use of bipolar stimulation,[31,38] common ground returns,[31] hexapolar returns (HP),[32,38–40] and quasimonopolar modes[32] with varying levels of success. Hexapolar stimulation, where the six electrodes surrounding each stimulating electrode are connected to each other and used a return or "guard," has been shown in previous studies to increase the specificity of activation in the retina and reduce electrical cross-talk.[31,40,41] However, this technique also results in a significant increase in stimulation threshold to elicit a cortical response,[31,32,38,41] which is consistent with studies showing increased perceptual thresholds for cochlear implant patients when receiving bipolar and TP stimulation.[27,33,42] While, at matched current levels, cortical activation has been shown to be reduced with HP stimulation compared to monopolar (MP) stimulation.[38] When responses have been compared at the same point along the dynamic range of each stimulation mode, no significant change in cortical spread has been found.[31] Also, reports from patients asked to compare the appearance of phosphenes generated by MP and HP stimulation have anecdotally suggested no evidence of size reduction with HP stimulation.[11] These results indicate that, while HP stimulation can increase retinal specificity, cortical specificity and beneficial perceptual effects have not yet been achieved.

Focused multipolar stimulation (FMP) is a technique pioneered in cochlear implants that uses simultaneous stimulation of multiple electrodes according to positive and negative weights to restrict the electric field and reduce the spread of neural activation.[43] Current weights are calculated by measuring the impedances between electrodes on the array and inferring the currents required to nullify voltage changes in the region surrounding a specific electrode.[43] This form of stimulation has been validated using cochlear implants in clinical and animal studies showing reduced intracochlear voltages,[43] increased spectral resolution in patients,[44] and reduced spread of neural activation in the inferior colliculus of cats.[33] However, the benefits of FMP stimulation have been restricted to a one-dimensional cochlear implant electrode array and to our knowledge this technique has not been assessed previously in the retina, or adapted for use on a two-dimensional electrode array. It is possible that the FMP technique may reduce the spread of neural activity over that found with HP stimulation. The HP return mode uses symmetrical negatively weighted flanking electrodes, while, as detailed in this study, FMP weights often show significant asymmetry. Failure to account for individual electrode impedances and the local tissue environment may, in part, explain why HP stimulation has not achieved reductions in spread of cortical activity.

We investigated the efficacy of FMP stimulation in reducing current spread and neural activation through recordings in the visual cortex (VC). Comparisons made between recordings taken from the VC of implanted cats in response to MP, HP and FMP stimulation were used to evaluate the relative effectiveness of these stimulation modes in producing focused activation.

## Methods

### Anesthesia and Surgery

All procedures were approved by the Bionics Institute Animal Research Ethics Committee (Project #14 304AB), complied with the ARVO Statement for Use of Animals in Ophthalmic and Vision Research, and were in accordance with the Australian Code of Practice for the Care Use of Animals for scientific purposes and with the National Institutes of Health (Bethesda, MD, USA) guidelines regarding the care and use of animals for experimental procedures. Normally sighted adult cats ($n = 6$) were anesthetized with ketamine (intramuscular [IM], 20 mg/kg) and xylazil (subcutaneous [SC], 2 mg/kg). Anesthesia was maintained over the experimental period for up to 3 days with a continuous intravenous (IV) infusion of sodium pentobarbitone (3–8 mg/kg/h). Respiration rate, end-tidal $CO_2$, blood pressure, and temperature were monitored consistently throughout the experiment and maintained at normal levels by adjusting the anesthetic flow rate. A continuous IV infusion of Hartmann's solution (sodium lactate, 2.5 mL/kg/h), and daily injections of dexamethasone (IM 0.1 mg/kg) and clavulox (SC 10 mg/kg) also were administered. Pupils were dilated by regular topical application of a mixture of phenylephrine hydrochloride (2.5%) and tropicamide (1%).

The suprachoroidal electrode array was similar to that which has been used in our previous work,[4,18] fabricated on a biocompatible silicon substrate and consisting of 42 platinum electrodes of 600-μm diameter spaced 1 mm from center to center. The implantation procedure is detailed in our previous studies.[18,19] Briefly, following a lateral canthotomy, scleral incision, and dissection of a pocket between the sclera and choroid, the array was inserted approximately 15 mm into the suprachoroidal space until the tip was beneath the area centralis. Electrical connections to the electrodes on the array were tested using an automated impedance monitoring software developed in LabVIEW (National Instruments, Austin, TX, USA) used in previous studies.[45] The animal was placed in a stereotaxic frame inside a darkened electrically shielded room. Visual inspection of the eye and fundus photographs were taken to determine the health of the eye and positioning of the array. A craniotomy then was performed spanning 15 mm rostral and 5 mm caudal from the interaural line, and 7 mm lateral from the sagittal suture on the side contralateral to the implanted eye, exposing the VC. The dura mater was excised carefully from the region. Using two parylene-based flexible platinum electrode arrays, electrically evoked potentials (EPs) in response to cathodic-leading biphasic charge-balanced current pulses (0–750 μA, 1 ms per phase) were mapped along the surface of the VC to determine the cortical region with the lowest evoked potential thresholds. Up to two planar "Utah" 36- ($6 \times 6$) or 60- ($6 \times 10$) channel penetrating microelectrode arrays (Blackrock Microsystems, Foxborough, MA, USA) were inserted in the regions of the VC with the lowest evoked potential thresholds to a depth of approximately 1 mm. The recording electrodes were separated by a distance of 400 μm and sampled approximately 7.2 and 4 $mm^2$ of the cortex for the 60- and 36-channel arrays, respectively. The size and number of electrode arrays used for each animal was determined by the prevalence and location of large blood vessels, as care was taken to minimize damage to these structures during insertion.

### Experimental Protocols

Electrical stimuli were generated with a 128-channel IZ2 stimulator (Tucker-Davis Technologies, Alachua, FL, USA). Due to the low maximum current output per channel (300 μA), each group of three channels was combined using a custom-built circuit board bringing the maximum functional number of

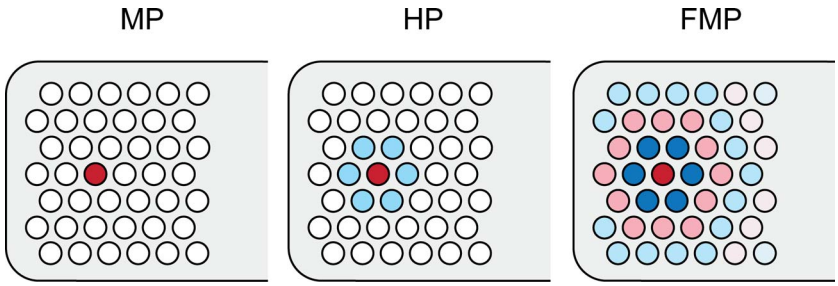


FIGURE 1. Illustration of electrode stimuli weights for MP, HP, and FMP stimulation techniques. Monopolar stimulation is represented as a single stimulating electrode. Hexapolar stimulation is shown to have negative weights on the six surrounding electrodes as these are used as return electrodes. Focused multipolar weights often presented as concentric rings of alternating positive and negative currents radiating from a central electrode. Each ring aims to cancel out the spread of current produced by the former.

combined stimulating channels to 42 and a maximum current output to 900 μA per combined channel. Each combined channel was connected directly to each electrode on the suprachoroidal array enabling independent simultaneous stimulation of all 42 electrodes. Three different modes of stimulation were trialed: (1) MP, whereby a single electrode was stimulated against an extraocular platinum return electrode inserted in to the conjunctiva of the implanted eye; (2) HP, where a single electrode was stimulated against the immediately surrounding "hexagon" of electrodes shorted together as a return; and (3) FMP, where all electrodes on the array were stimulated simultaneously against the extraocular platinum return electrode using positive and negative weights, with one of these electrodes chosen as the primary stimulating electrode (PSE) with a weight equal to 1. Pulses were presented at randomly varied currents ranging from zero to 750 μA in 50-μA steps at a repetition rate of 1 Hz. Each current step was repeated 10 times. Stimulus pulses were symmetrically biphasic with a 1000 μs phase width and 25 μs interphase gap. Thus, the maximum charge on each electrode was capped to 750 nC corresponding to the maximum charge density of 265 μC/cm, which is below the safe limit for gassing when using platinum electrodes.[46] Monopolar, HP, and positively weighted FMP stimulation pulses were presented cathodic-first, whereas negatively weighted FMP pulses were presented anodic first. For electrodes on the edge of the array without a full complement of six flanking electrodes, the HP mode only consisted of a partial ring of electrodes as a return directly adjacent to the stimulating electrode.

Focused multipolar weights were constructed using methods adapted from van den Honert and Kelsall[43] for the cochlear implant. A transimpedance matrix was constructed by stimulating each electrode in turn while recording voltages on every other electrode. To measure these voltages, the electrode array was connected to a 512 cross-point switch matrix (PXI 2523; National Instruments). Channels of the switch matrix also were connected to an isolated constant current stimulator and a digital multimeter (PXI 4072; National Instruments), allowing stimulation and voltage recording at any electrode site. Voltage waveforms were collected from every electrode in response to MP stimulation of every other electrode. Each trial was repeated 5 times and the waveforms were averaged. Transimpedance was calculated by dividing the voltage at the end of the first phase by the current, and arranged in a matrix where the columns corresponded to stimulating electrodes, and the rows to recording electrodes as follows:

$$Z_m = \begin{bmatrix} z_{E1,E1} & z_{E2,E1} & \cdots & z_{E42,E1} \\ z_{E1,E2} & z_{E2,E2} & \cdots & z_{E42,E2} \\ \vdots & \vdots & \ddots & \vdots \\ z_{E1,E42} & z_{E2,E42} & \cdots & z_{E42,E42} \end{bmatrix}$$

where $Z_{x,y}$ is the transimpedance between stimulating electrode $x$ and recording electrode $y$. Transimpedance measurements where the stimulating and recording electrodes are the same (on the diagonal of the matrix) could not be measured accurately due to the effects of polarization on the electrode carrying the current pulse. Therefore, these values were estimated using a linear extrapolation method adapted from van den Honert and Kelsall.[43] For a linear electrode array, such as the one used in a cochlear implant, values are estimated by taking the maximum among four values extrapolated from adjacent electrode pairs.[43] As the retinal array is two-dimensional, this was repeated in up to six directions, yielding, depending on electrode positioning, up to 12 extrapolated values. The maximum extrapolated value was chosen as the transimpedance of each stimulating electrode on the diagonal. The transimpedance matrix was averaged with its own transpose ($Z = Z_m + Z^T{}_m$) to decrease measurement noise and then inverted ($Y = Z^{-1}$), yielding a matrix of transadmittance values. Each column ($j$) of transadmittances then were normalized to the admittance value of the PSE ($Y_{j,j}$ on the diagonal of the matrix), to give the current weights to nullify the voltage at every electrode on the array except the PSE. These weights have been referred to as the phased array.[42] Focused multipolar weights typically presented as concentric circles of alternating positive and negative weights progressively approaching zero with greater distance from the PSE (see Fig. 1).

## Retinal Voltage Spread

To validate whether FMP stimulation was able to nullify voltages on surrounding electrodes, recordings from the retinal electrodes were used to assess the spread of voltage in the retina. For these recordings, single biphasic pulses at the maximum safe charge level of 750 nC, using MP or FMP stimulation, were applied to each electrode on the array and recordings were made from the directly surrounding electrodes. Due to hardware constraints, we were only able to record from a single electrode at a time. Therefore, a single pulse was applied to each electrode multiple times, but each time a recording was made from a different electrode. To eliminate the effects of electrode polarization during FMP stimulation, for each trial, the recording electrode was not included in the transimpedance calculations and was not stimulated as part of the phased array. While this technique did not use true FMP stimulation, as the phased array was not complete without the recording electrode, it provided a reasonable estimate of the voltage reduction capabilities of FMP stimulation. To quantify the difference between stimulation modes, the average of the summed voltage values of electrodes directly surrounding each PSE were compared between FMP and MP stimulation with a paired $t$-test. Due to time constraints, we did not record the voltage spread in

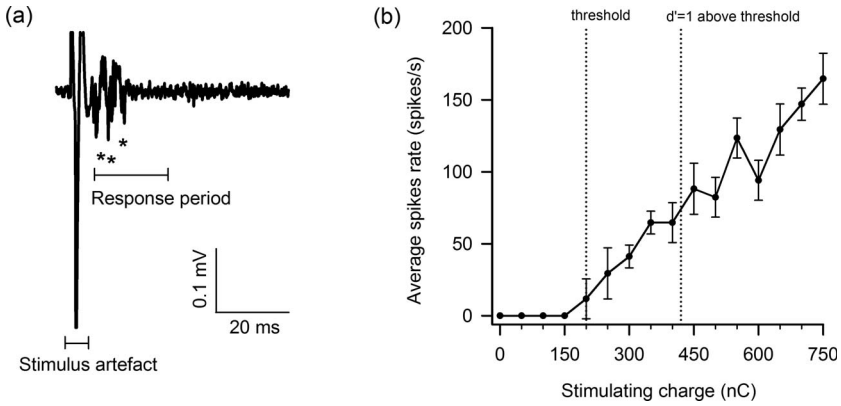


**Figure 2.** Examples of electrically evoked multiunit activity on a single cortical recording channel. (**a**) Recording of multiunit activity in response to stimulation of a single retinal electrode. Stimulation artefact and the recorded response are highlighted. *Detected spikes. (**b**) Input–output function of a single cortical channel in response to MP stimulation from a retinal electrode. The average number of recorded spikes is plotted against the stimulation charge. The *left-most dotted vertical line* denotes the threshold for that channel. The *right-most dotted vertical line* denotes the charge required on this channel to reach a discriminability index (*d'*) of 1 above threshold. *Error bars*: SEM.

response to HP stimulation. Simulations in previous studies have shown that HP stimulation results in a more discrete electric field than MP stimulation.[23,32]

## Cortical Data Analysis

Data recorded during the experiment were analyzed offline using custom scripts written in Igor Pro (Wavemetrics, Lake Oswego, OR, USA) and MATLAB (Mathworks, Natick, MA, USA). Signal artefacts from electrical stimulation were first removed using techniques described by Heffer and Fallon.[47] The signal was bandpass filtered (Butterworth filter; 0.3–5 Hz; order, 3) and background activity was estimated by calculating the root mean square (RMS) value every 60 seconds. Spikes on each cortical channel were timestamped if the signal exceeded −4 times the RMS value. Only spikes detected within a 3 to 20 ms window from stimulus onset were included in analyses. On some channels, there was a secondary response following the 3 to 20 ms window but we chose to include only the early response, as the secondary response is hypothesized to result from synaptically-mediated activation of retinal ganglion cells (RGCs) via bipolar cell activation as opposed to direct activation of RGCs, and to remain consistent with previous studies.[31,38,48] For each stimulating electrode, threshold was defined as the lowest current required to exhibit spike rates greater than the baseline spontaneous activity (typically near zero, See Fig. 2a) while showing a monotonic increase in spiking activity at all higher current levels (Fig. 2b) on any cortical channel. This differed from our previous studies where threshold has been defined as the current required to elicit 50% of the maximum spike rate observed on a channel.[31,39,49] An alternative threshold definition was used in this study as we found that, on many cortical channels, FMP and HP stimulation (and sometimes MP stimulation as shown in Fig. 2b) were not able to produce saturated responses even at the maximum safe charge used (750 nC), making it difficult to estimate dynamic range. As the previous threshold techniques relied on estimating the dynamic ranges in response to all stimulation modes to be known, we could not use this technique.

## Retinal and Cortical Selectivity

Selectivity was measured in the retina and cortex using the data recorded in the cortex from stimulation of the retinal electrodes. Prior studies have shown that different return modes can result in varying thresholds, indicating that cortical spread should not be compared at matched stimulus intensity, but rather at matched "brightness" levels. Our previous studies have used percent of maximum spike rate as a way of comparing responses at the same point along the dynamic range. However, as many recording channels failed to reach saturation of spiking activity, in this study we quantified the growth of neural response by calculating the discrimination index (*d'*) of spike rates at each current level compared to spiking activity at threshold. This was achieved using methodology derived from signal detection theory.[50] A receiver operator curve was constructed for each channel using the spike rates for threshold and suprathreshold stimulus intensities. The area underneath the curve was converted to a standard deviate and multiplied by $\sqrt{2}$ to calculate *d'*. The current level at which a channel reached $d' = 1$ above threshold was derived through linear interpolation. When estimating retinal selectivity, for each cortical channel, a best retinal electrode (BRE) was defined as the stimulating electrode that required the least current to elicit a spike rate on that cortical channel that yielded $d' = 1$ above threshold. The *d'* values elicited on that cortical channel in response to the other retinal electrodes at that same current also were calculated and placed in 1-mm width bins (corresponding to the distance between adjacent retinal electrodes), then plotted as a function of distance from the BRE. To represent the worst spread, in each distance bin the maximum *d'* value was used for further analyses. These maximum binned values then were averaged across all cortical channels and compared across stimulation modes.

Cortical selectivity was estimated using a similar approach. A best cortical electrode (BCE) was determined for each stimulating retinal electrode. The BCE was defined as the cortical channel that required the smallest current to elicit a spike rate that yielded $d' = 1$ above threshold. The *d'* values of the other cortical channels elicited by that same current then were calculated as a function of distance from BCE (in mm). These *d'* values then were placed in 0.4-mm wide (corresponding to the distance between adjacent cortical electrodes) bins and the maximum values of each bin were averaged over the plots for all retinal electrodes and compared between stimulation modes. Statistical analyses were performed using SigmaPlot (Systat Software, San Jose, CA, USA). Comparison of retinal electrode voltage spread between MP and FMP

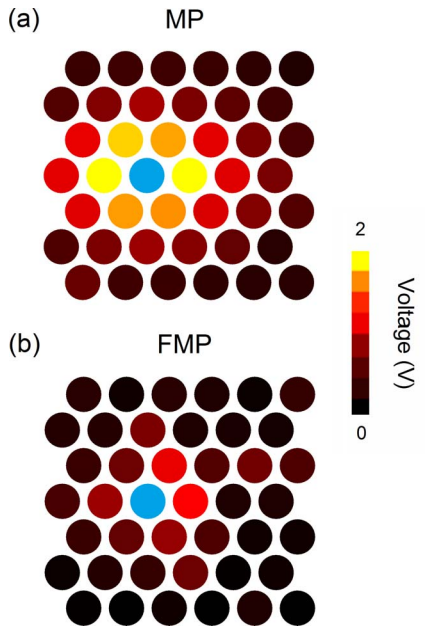


FIGURE 3. Example of voltages recorded on the suprachoroidal array in response to MP and FMP stimulation applied to the same electrode (*highlighted blue*). Each *circle* represents an electrode on the array. The *color* of the *dot* represents voltage as indicated by the *color bar* on the *left*. Voltages of nearby electrodes appear to be higher for MP than for FMP stimulation. Note, for FMP stimulation when recording a voltage on a given electrode, all other electrodes were stimulated using their corresponding current weights.

stimulation was performed using a paired *t*-test. A 1-way ANOVA was used to compare threshold differences among the three stimulation modes and post hoc differences were calculated using the Tukey test. Differences in cortical and retinal selectivity were determined with 2-way ANOVAs, using binned distance and stimulus mode as factors, with post hoc differences calculated using the Tukey test.

## RESULTS

### Retinal Voltage Spread

When using FMP stimulation, the calculated stimulation weights of electrodes immediately surrounding the PSE were greatly asymmetrical, unlike HP stimulation. Excluding electrodes that were not surrounded by a full ring of six electrodes, the average FMP weight applied to immediately adjacent electrodes was –0.237 ± 0.017 (±SEM), which is significantly higher (paired *t*-test, $P < 0.001$) than the average weight for HP stimulation at –0.167, assuming current was distributed evenly across the return electrodes during HP stimulation.

Voltage recordings were obtained from 224 surrounding electrodes in response to 39 stimulating electrodes. Voltages recorded at these sites were significantly reduced when FMP stimulation was used (paired *t*-test, $P < 0.001$), with a drop from 1.88 ± 0.12 V (mean ± SEM) for MP stimulation to 0.38 ± 0.18 V for FMP stimulation (shown in Figs. 3, 4), representing an average 80% drop in voltage. These results suggested that the adaptation of FMP stimulation from a one-dimensional cochlear array to a two-dimensional retinal array was successful and that FMP stimulation successfully restricted the electric field in the retina.

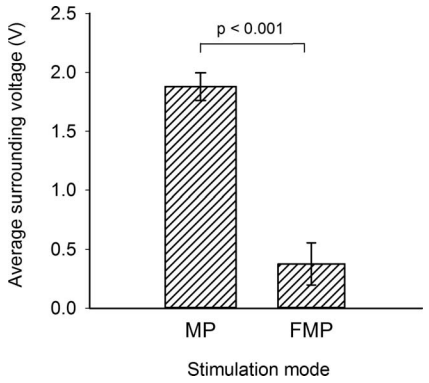


FIGURE 4. Average voltage of electrodes directly adjacent to each PSE during MP and FMP stimulation. Average surrounding voltages were significantly lower for FMP stimulation when compared to MP stimulation (paired *t*-test, $P < 0.001$). *Error bars*: SEM.

### Cortical Thresholds

Cortical responses were collected in response to stimulation of 150 retinal electrodes using the three modes (MP, HP, and FMP) across all six animals. It was not possible during the experiments to stimulate all 42 electrodes on each array due to time limitations. The number of retinal electrodes that elicited a response on at least one cortical channel reaching $d' = 1$ above threshold was 111 for MP stimulation, 93 for HP stimulation, and 90 for FMP stimulation. Only the 73 retinal electrodes that elicited at least one cortical channel to reach $d' = 1$ above threshold using all stimulation modes were included in analysis. Of 12,516 recording channels in the VC, 8173 channels recorded activity reaching $d' = 1$ above threshold for at least one stimulating electrode (4296 sites for MP, 1547 sites for HP, and 1330 sites for FMP). A total of 195 channels recorded spike rates that reached $d' = 1$ above threshold in response to at least one retinal electrode for all three stimulation modes.

Significant differences in cortical activation thresholds were observed between the two focusing techniques and MP stimulation. Average thresholds for HP and FMP stimulation (255 ± 20 and 296 ± 20 nC, respectively) were significantly higher than MP stimulation (173 ± 17 nC) (1-way ANOVA, $P < 0.001$) as shown in Figure 5. No difference was found between HP and FMP stimulation.

### Retinal Selectivity

There was a significant reduction in retinal activation spread when HP and FMP stimulation were used compared to MP stimulation (2-way ANOVA, $P < 0.001$, Tukey post hoc test). Figure 6 shows an example of the $d'$ values calculated on a single cortical channel when stimulation is applied to each electrode at the lowest current to reach $d' = 1$ above threshold on the BRE, using each stimulation mode. In this example, the responses elicited on the cortical channel by electrodes adjacent to the BRE were smaller when HP and FMP stimulation were applied than when MP stimulation was applied. When averaging across all data, there was a significant interaction between distance from BRE and stimulation mode (2-way ANOVA, $P < 0.001$). Figure 7 shows that activity elicited in the cortex by stimulating electrodes within 2 mm of the BRE was significantly reduced (2-way ANOVA, $P < 0.001$) with HP and FMP stimulation compared to MP stimulation, with no significant difference between the stimulation modes beyond 2 mm ($P > 0.05$). There also was

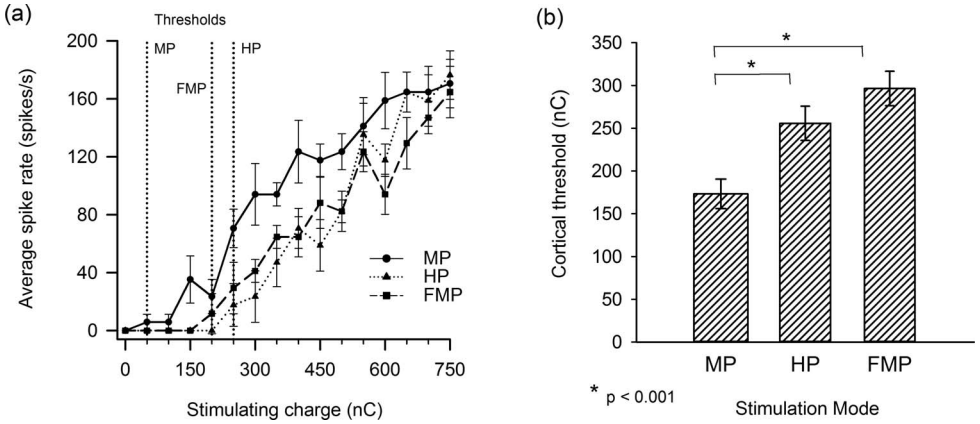


**Figure 5.** (**a**) Input–output function on a single cortical channel in response to MP, HP, and FMP stimulation showing the thresholds for each mode. (**b**) Average threshold values for MP, HP, and FMP stimulation ($n = 150$). Threshold for a retinal electrode was determined as the lowest current required to elicit spiking activity above spontaneous activity on any cortical recording channel. There was a significant increase in thresholds for HP and FMP stimulation when compared to MP stimulation (1-way ANOVA, $P < 0.001$). However, there was no difference between HP and FMP stimulation. *Error bars*: SEM.

no significant difference in activity elicited between HP and FMP stimulation ($P > 0.05$).

## Cortical Selectivity

At the current required to reach $d' = 1$ above threshold on the BCE, a significant reduction in cortical activation spread was observed for HP and FMP stimulation modes over MP stimulation. An example of activity recorded with a $6 \times 10$ planar recording array in response to the three stimulation modes applied to the same retinal electrode is shown in Figure 8a. The spread of activation in the cortex in response to MP stimulation was far broader than that elicited by HP and FMP stimulation in this example. Maximum $d'$ values of channels surrounding the BCE were lower for HP and FMP than for MP stimulation in this example (Fig. 8b). Average cortical selectivity across all stimulating electrodes indicated a significantly greater reduction in the spread of cortical activation for

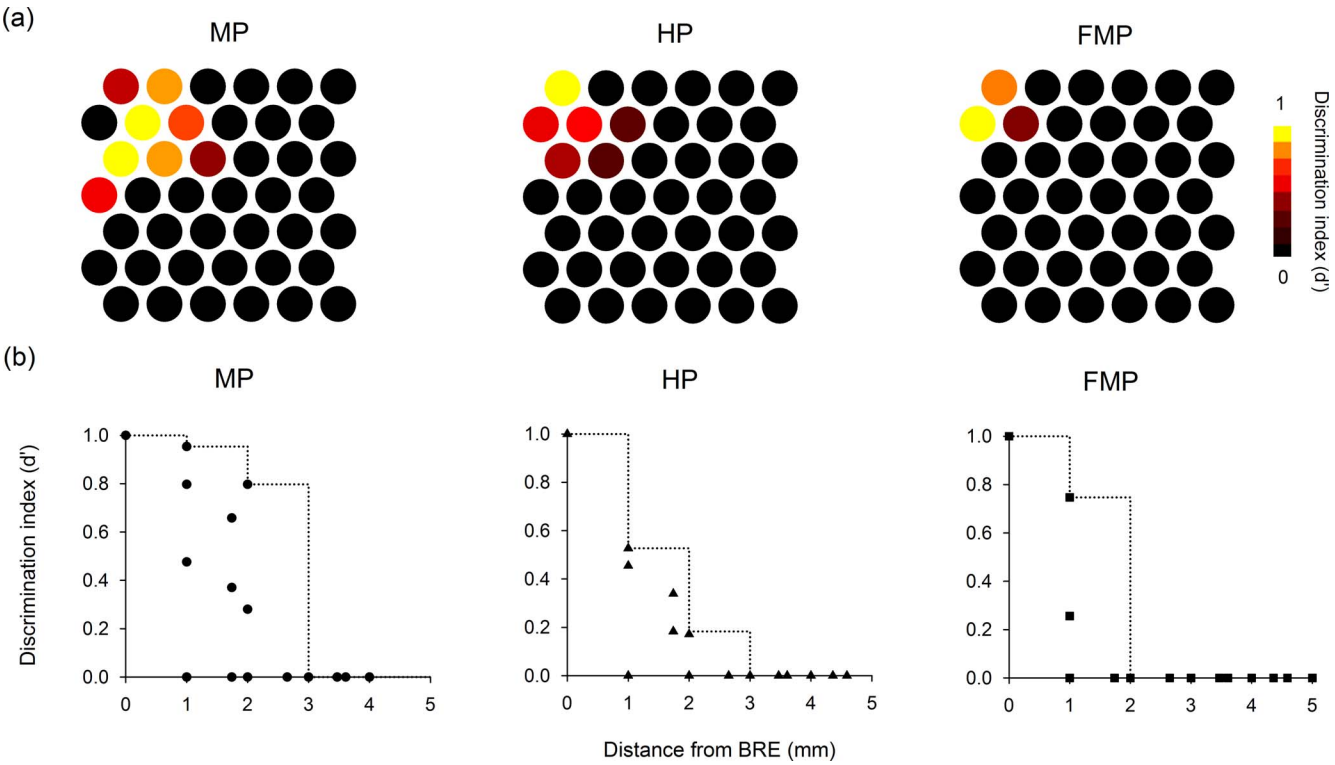


**Figure 6.** (**a**) Examples of retinal selectivity maps for a single cortical channel when MP, HP, and FMP stimulation were used. Maps show $d'$ above threshold values elicited on the same cortical channel when electrodes were stimulated at the current level required to reach $d' = 1$ above threshold on the BRE. Monopolar stimulation elicited responses on the cortical channel to stimulation of a broader range of retinal electrodes than for HP and FMP stimulation. (**b**) Examples of selectivity plots for responses to MP, HP, and FMP constructed from the data shown in (**a**). The $d'$ values are plotted against the distance of the stimulating electrode from the BRE. Electrodes that did not result in a response on the cortical channel at any current level are excluded. The *dotted line* shows the running maximum of each 1 mm wide bin.

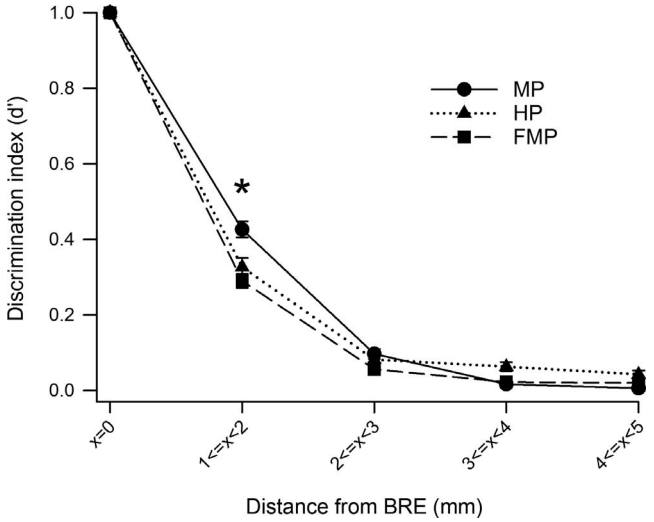


FIGURE 7. Average of the maximum *d'* values elicited on cortical channels by retinal electrodes, at the current required to reach $d' = 1$ above threshold on the BRE for each stimulation mode. All stimulation modes showed a steady decline in discriminability above threshold with increasing distance from the BRE. Hexapolar and FMP stimulation showed a significantly steeper decline for the first bin (indicated by an *asterisk*) when compared to MP stimulation (2-way ANOVA, $P < 0.001$). No significant difference was found between HP and FMP stimulation (2-way ANOVA, $P > 0.05$). *Error bars*: SEM.

HP and FMP stimulation than for MP stimulation (Fig. 9; 2-way ANOVA, $P < 0.001$, Tukey post hoc test), and unlike retinal selectivity, there was no significant interaction between distance and stimulation mode and no differences between HP and FMP stimulation ($P > 0.05$).

## Discussion

We investigated the effectiveness of FMP stimulation in reducing the spread of neural activation in the retina and VC compared to MP and HP stimulation. The main finding of this study was that FMP and HP stimulation resulted in significantly restricted spatial spread of neural activation in the retina and VC when compared to MP stimulation, albeit requiring higher charge levels for FMP and HP stimulation to reach neural activation thresholds. Contrary to our initial hypothesis, no differences in any of the measures were found between FMP and HP stimulation.

### Retinal Voltage Spread

Focused multipolar stimulation showed significantly lower voltages on retinal electrodes directly adjacent to the PSE compared to MP stimulation, implying a decrease in current spread in the retina. The restriction of current spread is consistent with computational models for one-dimensional FMP[43,51] and indicates that FMP also is effective when applied to a two-dimensional electrode array. These data suggested that a reduction in neural recruitment with FMP stimulation can be likely and that more discrete responses would be elicited downstream in the visual pathway. Being able to reduce the spread of the electric field in the retina also suggests that channel interaction may be reduced with a retinal prosthesis when using FMP stimulation.[24,25,30] Focused multipolar stimulation has been shown in the cochlear implant to significantly reduce the effects of channel interaction on inferior colliculus activation.[25] This has important implications for stimulation strategies that would employ simultaneous stimulation of multiple electrodes.[24,30,52] Although we did not measure voltage spread for HP stimulation, it is likely that it also would be able to reduce the effects of channel interaction as it had similar effects on retinal and cortical selectivity as did FMP. It has been shown previously that TP stimulation in the cochlea (analogous to HP stimulation in our study) also was able to reduce channel interaction to the same level as that of FMP stimulation.[25]

### Cortical Thresholds

Activation thresholds in the VC for HP and FMP stimulation were significantly higher than those for MP stimulation. This is consistent with previous work in the retina and cochlea showing that FMP and discrete return modes, such as HP,[11,31,32,41,53] TP,[27,33,34] and bipolar[54] stimulation, require higher charge levels to elicit comparable responses. However, compared to previous work with HP stimulation in the retina, threshold differences between MP and HP stimulation were not as pronounced.[11,31] This study showed a 32% increase in threshold whereas our previous preclinical study reported over 100% increase. The smaller threshold increase is likely due to methodologic differences. In particular, the difference in threshold definition, as the previous study defined threshold at 50% of the maximum observed spike rate,[31] and the different geometries of the electrode arrays used.

The increased thresholds observed may be due to the more restricted electric field with HP and FMP stimulation being unable to penetrate through to the retina. Current shunting via the highly conductive choroidal blood vessels also may contribute.[54,55] Higher thresholds may have consequences in a clinical scenario as higher charge levels are more likely to be damaging to the surrounding tissue. The fact that many channels did not reach a saturation of responses at the maximum safe charge injection limits also is concerning as the focusing methods may not be able to reach the same levels of brightness as MP stimulation. A variation of FMP has been trialed in a cochlear implant study termed partial-FMP to address the increase in thresholds.[34] In this method, weights are calculated the same way; however, a multiplier is applied to the diagonal values of the transimpedance matrix, thereby affording a greater ratio of current to the PSE.[34] This method is similar to other focusing methods, such as partial-TP[42] and quasimonopolar stimulation.[32,56] Using this method, lower thresholds could be attained possibly without compromising on selectivity, allowing for titration of the two factors.[34] It is likely that a partial-FMP approach could be applied to the retina to compensate for the increased thresholds; however, inevitably there may always be a trade-off with threshold and selectivity.

### Retinal and Cortical Selectivity

Retinal and cortical selectivity for HP and FMP stimulation was shown to be significantly higher than for MP stimulation. This shows that the two focusing techniques were effective at restricting the region of neural recruitment in the retina and, by extension, evoked activity in the VC. There was no significant difference between HP and FMP stimulation in terms of retinal or cortical selectivity, suggesting that this application of FMP stimulation did not result in more focused stimulation than using a HP return mode. Also with retinal selectivity, there were no significant differences at 2 mm or further from the BRE among the three modes. However, note that *d'* values determined for all modes at these distances often were very low, as even MP stimulation would seldom spread far at these current levels. This is consistent with our previous

Investigative Ophthalmology & Visual Science

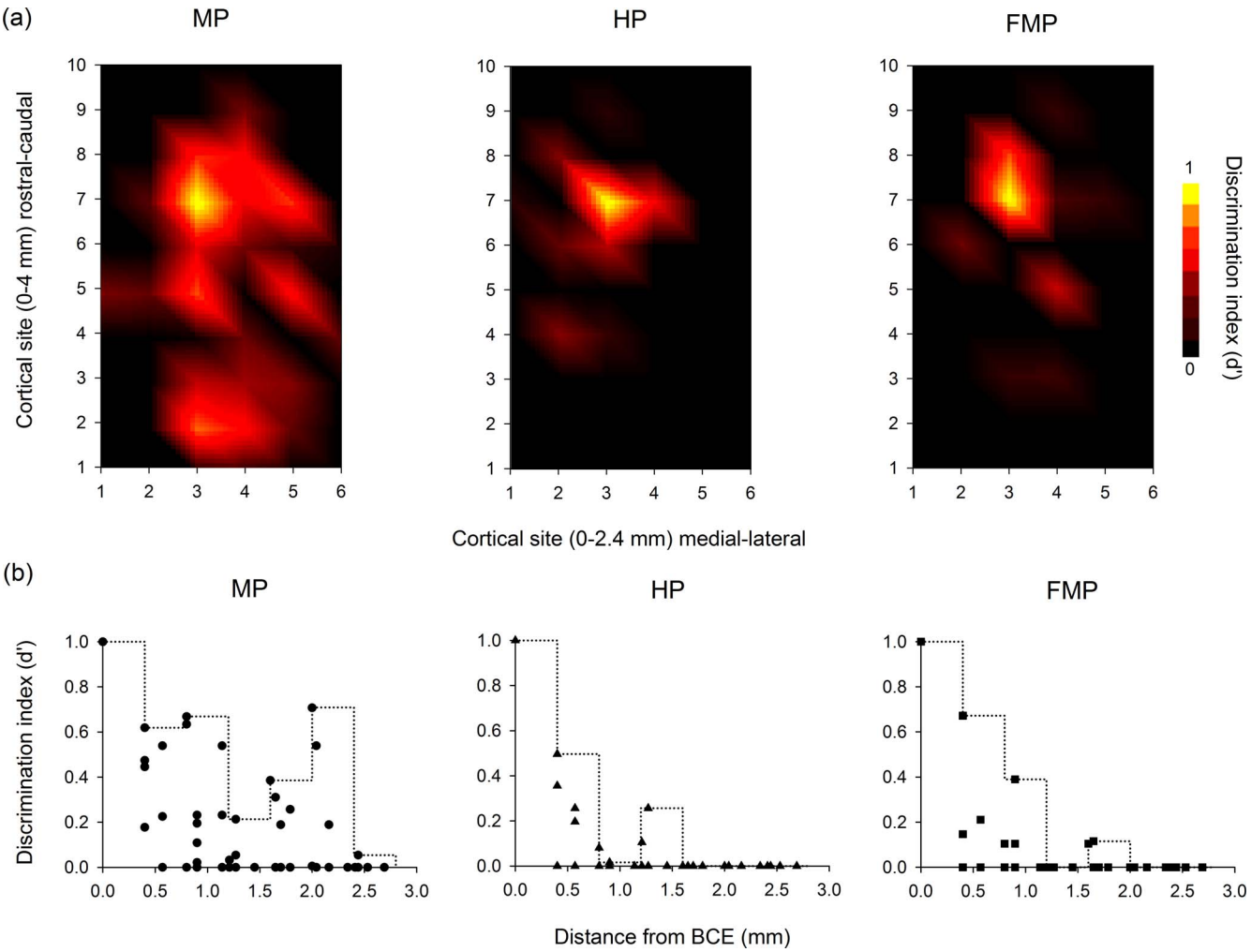


FIGURE 8. (**a**) Examples of response patterns on the cortical recording array (6 × 10 planar) for MP, HP, and FMP stimulation. Colors represent the *d'* above threshold of responses at the current required to reach *d'* = 1 above threshold on the BCE. Monopolar stimulation elicited a broader region of activation than HP and FMP stimulation. (**b**) Examples of selectivity plots for responses to MP, HP, and FMP constructed from the data shown in (**a**). The *d'* above threshold as a function of distance from BCE. Electrodes that did not reach threshold at any current level were excluded. The *dotted line* shows the running maximum of each 0.4 mm wide bin.

study where responses on a given cortical channel were much less when an electrode 2 mm or further from the BRE was stimulated.[31] Based on the average receptive field of a cat cortical neuron, 1.6°, it is unlikely that a single cortical site would receive projections from an area more than 2 mm away from the BRE.[57]

Based on our cortical selectivity measures, we can estimate that stimulation applied to a single site yielded evoked activity in 2.4 mm of the cortex for MP stimulation, and 1.6 mm of cortex for HP and FMP stimulation (defined as the bin distance where *d'* values drop consistently below 0.1; see Fig. 9). Using a cortical magnification factor of 0.707 mm of cortex/degree of visual field for an eccentricity of 10°, as defined by Tusa et al.,[7] these regions of activation equate to approximately 1.69° and 1.13° of visual angle, respectively, indicating that a higher degree of resolution could be achieved with HP and FMP stimulation.

In regards to HP stimulation, the results of this study are partially consistent with our previous study.[31] Hexapolar stimulation has been shown in previous work to restrict retinal activation.[31,41] However, it was shown to have no impact on cortical selectivity[31] and anecdotally did not produce smaller phosphenes in patients compared to MP stimulation.[11] One explanation for this is the method used to match intensity levels. The previous study in animals compared responses at the same point along the dynamic range of neural responses, determined by percent of maximum spike rate,[31] as opposed to this study, where we converted responses into *d'* values to assess the level of discriminability above threshold to simulate a matched "brightness" level in the brain. Also, in patients, while phosphenes were compared at the same level above relative thresholds, these amplitudes may not have been at the same point along the perceptual dynamic range, which would have been expected to be different between MP and HP stimulation, based on what we showed in our previous preclinical study.[31] This highlights the importance of the method used to determine selectivity, electrophysiologically and clinically, when using different stimulation modes. While we have used two different approaches in our laboratory, clinically, the ideal approach would be to compare phosphene sizes at brightness-matched levels. However, as brightness and phosphene size are known to co-vary with stimulus amplitude, it may be sufficient to compare the degree of growth in both measures when comparing different stimulation modes, where FMP and HP stimulation could be

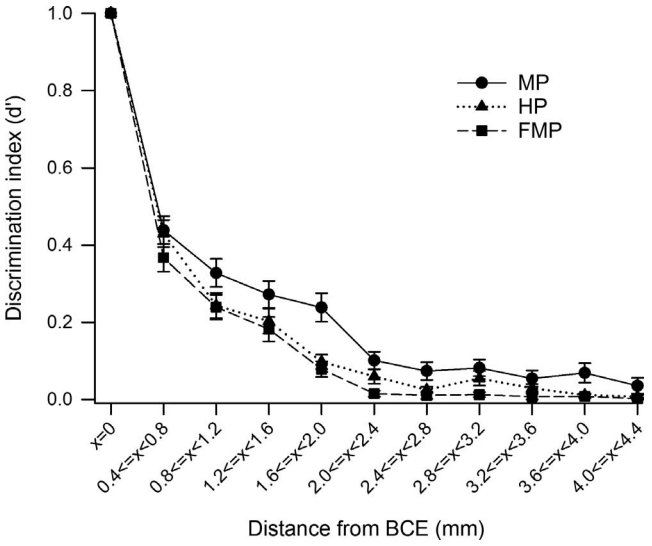


FIGURE 9. Average of the maximum *d'* values of cortical channels at the current required to reach $d' = 1$ above threshold on the BCE for each stimulation mode. All stimulation modes showed a steady decline in discriminability as the distance from BCE increased. Hexapolar and FMP stimulation shows a significantly steeper decline when compared to MP stimulation, with no significant interactions between distance and stimulation mode (2-way ANOVA, $P < 0.001$). No significant difference was found between HP and FMP stimulation (2-way ANOVA, $P < 0.001$). *Error bars*: SEM.

expected to elicit a smaller degree of growth compared to MP stimulation. Another explanation for the divergence in selectivity results between this study and our previous preclinical study is the difference in electrode geometry. Electrodes used in this study had a greater diameter than the previous study; however, they maintained the same distance center-to-center.[31] This change may account for the different results as reduced edge-to-edge distance between electrodes may have resulted in greater voltage reduction with a HP return arrangement compared to our previous study.

A somewhat surprising finding in our study was that FMP weights applied to channels immediately adjacent to the PSE were significantly higher than estimated HP weights, especially since we found no differences in our cortical measures. This diverges from recordings taken from cochlear implants where the weights of flanking electrodes typically are calculated to be approximately –0.5, dividing current equally between the two channels.[43,58,59] This possibly could be due to the differences between the electrode-tissue interface in the cochlea and the suprachoroidal space. Intracochlear electrodes often are in contact with fluid of relatively consistent impedance whereas the retinal electrodes are in contact with the choroid, which is comprised of a heterogeneous assortment of connective tissue and blood vessels.[54,55] However, this does indicate that FMP stimulation is not merely replicating HP stimulation. While this study does not detect any significant functional difference between the two modes, it is possible that there would be perceptual differences that we are unable to determine using our analysis method.

Overall, our results indicated that HP and FMP stimulation techniques are capable of restricting the spread of neural activation in the retina and VC, which would be expected to result in the perception of more discrete phosphenes when compared either at the same point along their perceptual dynamic range or at an equivalent brightness level compared to MP stimulation.

### Future Studies

This study demonstrated that HP and, for the first time to our knowledge, FMP stimulation is capable of restricting the spread of activation in two dimensions in the retina. Firstly, this has important implications for stimulation strategies requiring simultaneous stimulation of electrodes. It has been shown previously that channel interaction can be minimized on a linear intracochlear electrode array using TP and FMP stimulation.[25] It also has been shown that channel interactions can be reduced in the retina using HP stimulation.[40] Further investigation in the use of these current focusing techniques in reducing electrical crosstalk in the retina could be of great benefit.

Secondly, there are a number of differences between the state of the feline eye in this study and the likely state of a retinal prosthesis patient's eye that may impact the translation of these findings to patients. Our experiments were conducted following an acute implantation of the suprachoroidal device. In patients, a number of long-term morphologic changes occur in the eye following implantation, such as chronic inflammation and fibrosis, that are not represented in this study.[18] Further studies in long-term implanted animals would provide a more accurate understanding of the efficacy of HP and FMP stimulation in a more representative scenario. Also, the animals used during this study were sighted cats with intact healthy retinas. At least for the near future, the intended recipients for a retinal prosthesis currently are patients with severe photoreceptor loss and associated remodeling of the remaining retinal circuitry. Our previous work in a feline model[60] of photoreceptor degeneration indicates that activation spread is largely unchanged, however it is possible that the increased thresholds of the focusing techniques may have a more pronounced effect in a blind recipient. Further studies in an animal model of retinal degeneration would give a much clearer indication on the effects of HP and FMP stimulation on the blind retina.

## CONCLUSIONS

This study showed, for the first time to our knowledge, that current focusing techniques reduced voltage spread and neural activation in the retina and, by extension, the spread of evoked activity in the VC, compared to traditional MP stimulation at the expense of higher thresholds. To our knowledge, this also is the first instance of FMP being attempted with a two-dimensional electrode array. No significant differences were observed between the two focusing techniques. Clinical application of these techniques would be expected to result in smaller phosphenes; thus, reducing phosphene overlap between electrodes and increasing visual resolution for retinal prosthesis recipients. Further study in long-term implanted blind feline models could give a clearer insight into the translational benefit of these techniques.

### *Acknowledgments*

The authors thank Stephanie Epp, Ceara McGowan, Dimitra Stathopoulos, Alison Neil, Rodney Millard, Kerry Halupka, Alexia Saunders, and Evgeni Sergeev for technical assistance; and Penny Allen and Chi Luu for implanting the suprachoroidal devices.

Supported by the National Health and Medical Research Council (NHMRC) Project Grant (GNT1063093). The Bionics Institute acknowledges the support it receives from the Victorian Government through its Operational Infrastructure Support Program.

Disclosure: **T.C. Spencer**, None; **J.B. Fallon**, P; **P.C. Thien**, None; **M.N. Shivdasani**, P

## References


1. Hartong DT, Berson EL, Dryja TP. Retinitis pigmentosa. *Lancet*. 2006;368:1795–1809.
2. Fujikado T, Kamei M, Sakaguchi H, et al. Testing of semichronically implanted retinal prosthesis by suprachoroidal-transretinal stimulation in patients with retinitis pigmentosa. *Invest Ophthalmol Vis Sci*. 2011;52:4726–4733.
3. Humayun MS, Dorn JD, da Cruz L, et al. Interim results from the international trial of Second Sight's visual prosthesis. *Ophthalmology*. 2012;119:779–788.
4. Ayton LN, Blamey PJ, Guymer RH, et al. First-in-human trial of a novel suprachoroidal retinal prosthesis. *PLoS One*. 2014;9:e115239.
5. Zrenner E, Bartz-Schmidt KU, Benav H, et al. Subretinal electronic chips allow blind patients to read letters and combine them to words. *Proc Biol Sci*. 2011;278:1489–1497.
6. Shepherd RK, Shivdasani MN, Nayagam DA, Williams CE, Blamey PJ. Visual prostheses for the blind. *Trends Biotechnol*. 2013;31:562–571.
7. Tusa R. The retinotopic organization of area 17 (striate cortex) in the cat. *J Comp Neurol*. 1978;177:213–235.
8. Santos A, Humayun MS, de Juan ED Jr, Marsh MJ, Klock IB, Milam AH. Preservation of the Inner Retina in Retinitis Pigmentosa. *Arch Ophthalmol*. 1997;115:511–515.
9. Jones BW, Watt CB, Frederick JM, et al. Retinal remodeling triggered by photoreceptor degenerations. *J Comp Neurol*. 2003;464:1–16.
10. Ahuja AK, Dorn JD, Caspi A, et al. Blind subjects implanted with the Argus II retinal prosthesis are able to improve performance in a spatial-motor task. *Br J Ophthalmol*. 2011;95:539–543.
11. Shivdasani MN, Sinclair NC, Dimitrov PN, et al. Factors affecting perceptual thresholds in a suprachoroidal retinal prosthesis. *Invest Ophthalmol Vis Sci*. 2014;55:6467–6481.
12. De Balthasar C, Patel S, Roy A, et al. Factors affecting perceptual thresholds in epiretinal prostheses. *Invest Ophthalmol Vis Sci*. 2008;49:2303–2314.
13. Klauke S, Goertz M, Rein S, et al. Stimulation with a wireless intraocular epiretinal implant elicits visual percepts in blind humans. *Invest Ophthalmol Vis Sci*. 2011;52:449–455.
14. Wilke R, Gabel VP, Sachs H, et al. Spatial resolution and perception of patterns mediated by a subretinal 16-electrode array in patients blinded by hereditary retinal dystrophies. *Invest Ophthalmol Vis Sci*. 2011;52:5995–6003.
15. Rizzo JF, Wyatt J, Loewenstein J, Kelly S, Shire D. Perceptual efficacy of electrical stimulation of human retina with a microelectrode array during short-term surgical trials. *Invest Ophthalmol Vis Sci*. 2003;44:5362–5369.
16. Rizzo JF, Wyatt J, Loewenstein J, Kelly S, Shire D. Methods and perceptual thresholds for short-term electrical stimulation of human retina with microelectrode arrays. *Invest Ophthalmol Vis Sci*. 2003;44:5355–5361.
17. Stingl K, Bartz-Schmidt KU, Besch D, et al. Artificial vision with wirelessly powered subretinal electronic implant alpha-IMS. *Proc Biol Sci*. 2013;280:20130077.
18. Villalobos J, Nayagam DA, Allen PJ, et al. A wide-field suprachoroidal retinal prosthesis is stable and well tolerated following chronic implantation. *Invest Ophthalmol Vis Sci*. 2013;54:3751–3762.
19. Saunders AL, Williams CE, Heriot W, et al. Development of a surgical procedure for implantation of a prototype suprachoroidal retinal prosthesis. *Clin Exp Ophthalmol*. 2014;42:665–674.
20. Yamauchi Y, Franco LM, Jackson DJ, et al. Comparison of electrically evoked cortical potential thresholds generated with subretinal or suprachoroidal placement of a microelectrode array in the rabbit. *J Neural Eng*. 2005;2:S48–S56.
21. Fujikado T, Morimoto T, Kanda H, et al. Evaluation of phosphenes elicited by extraocular stimulation in normals and by suprachoroidal-transretinal stimulation in patients with retinitis pigmentosa. *Graefe's Arch Clin Exp Ophthalmol*. 2007;245:1411–1419.
22. Chen SC, Suaning GJ, Morley JW, Lovell NH. Simulating prosthetic vision: II. Measuring functional capacity. *Vision Res*. 2009;49:2329–2343.
23. Wilke RGH, Moghadam GK, Lovell NH, Suaning GJ, Dokos S. Electric crosstalk impairs spatial resolution of multi-electrode arrays in retinal implants. *J Neural Eng*. 2011;8:046016.
24. Horsager A, Greenberg RJ, Fine I. Spatiotemporal interactions in retinal prosthesis subjects. *Invest Ophthalmol Vis Sci*. 2010;51:1223–1233.
25. George SS, Shivdasani MN, Wise AK, Shepherd RK, Fallon JB. Electrophysiological channel interactions using focused multipolar stimulation for cochlear implants. *J Neural Eng*. 2015;12:066005.
26. Boëx C, de Balthasar C, Kós M-I, Pelizzone M. Electrical field interactions in different cochlear implant systems. *J Acoust Soc Am*. 2003;114:2049.
27. Bierer JA. Threshold and channel interaction in cochlear implant users: evaluation of the tripolar electrode configuration. *J Acoust Soc Am*. 2007;121:1642–1653.
28. Gerhardt M, Alderman J, Stett A. Electric field stimulation of bipolar cells in a degenerated retina–a theoretical study. *IEEE Trans Neural Syst Rehabil Eng*. 2010;18:1–10.
29. Lovell NH, Dokos S, Cheng E, Suaning GJ. Simulation of parallel current injection for use in a vision prosthesis. In: *Conference Proceedings: Second International IEEE EMBS Conference on Neural Engineering*. Piscatawey, NJ: IEEE; 2005:458–461.
30. Horsager A, Boynton GM, Greenberg RJ, Fine I. Temporal interactions during paired-electrode stimulation in two retinal prosthesis subjects. *Invest Ophthalmol Vis Sci*. 2011;52:549–557.
31. Cicione R, Shivdasani MN, Fallon JB, et al. Visual cortex responses to suprachoroidal electrical stimulation of the retina: effects of electrode return configuration. *J Neural Eng*. 2012;9:036009.
32. Matteucci PB, Chen SC, Tsai D, et al. Current steering in retinal stimulation via a quasimonopolar stimulation paradigm. *Invest Ophthalmol Vis Sci*. 2013;54:4307–4320.
33. George SS, Wise AK, Shivdasani MN, Shepherd RK, Fallon JB. Evaluation of focused multipolar stimulation for cochlear implants in acutely deafened cats. *J Neural Eng*. 2014;11:065003.
34. George SS, Wise AK, Fallon JB, Shepherd RK. Evaluation of focused multipolar stimulation for cochlear implants in long-term deafened cats. *J Neural Eng*. 2015;12:036003.
35. Berenstein CK, Mens LHM, Mulder JJS, Vanpoucke FJ. Current steering and current focusing in cochlear implants: comparison of monopolar, tripolar, and virtual channel electrode configurations. *Ear Hear*. 2008;29:250–260.
36. Zwolan TA, Kileny PR, Ashbaugh C, Telian SA. Patient performance with the Cochlear Corporation "20+2" implant: bipolar versus monopolar activation. *Otol Neurotol*. 1996;17:717–723.
37. Pfingst BE, Zwolan TA, Holloway LA. Effects of stimulus configuration on psychophysical operating levels and on speech recognition with cochlear implants. *Hear Res*. 1997;112:247–260.
38. Wong YT, Chen SC, Seo JM, Morley JW, Lovell NH, Suaning GJ. Focal activation of the feline retina via a suprachoroidal electrode array. *Vision Res*. 2009;49:825–833.


Investigative Ophthalmology & Visual Science

39. Shivdasani MN, Fallon JB, Luu CD, et al. Visual cortex responses to single- and simultaneous multiple-electrode stimulation of the retina: implications for retinal prostheses. *Invest Ophthalmol Vis Sci*. 2012;53:6291–6300.
40. Matteucci PB, Barriga-Rivera A, Eiber CD, Lovell NH, Morley JW, Suaning GJ. The effect of electric cross-talk in retinal neurostimulation. *Invest Ophthalmology Vis Sci*. 2016;57: 1031.
41. Habib AG, Cameron MA, Suaning GJ, Lovell NH, Morley JW. Spatially restricted electrical activation of retinal ganglion cells in the rabbit retina by hexapolar electrode return configuration. *J Neural Eng*. 2013;10:036013.
42. Wu C-C, Luo X. Current steering with partial tripolar stimulation mode in cochlear implants. *J Assoc Res Otolaryngol*. 2013;14:213–231.
43. van den Honert C, Kelsall DC. Focused intracochlear electric stimulation with phased array channels. *J Acoust Soc Am*. 2007;121:3703–3716.
44. Smith ZM, Parkinson WS, Long CJ. Multipolar current focusing increases spectral resolution in cochlear implants. *Conf Proc IEEE Eng Med Biol Soc*. 2013;2796–2799.
45. John SE, Shivdasani MN, Leuenberger J, et al. An automated system for rapid evaluation of high-density electrode arrays in neural prostheses. *J Neural Eng*. 2011;8:036011.
46. Leung RT, Shivdasani MN, Nayagam DAX, Shepherd RK. In vivo and in vitro comparison of the charge injection capacity of platinum macroelectrodes. *IEEE Trans Biomed Eng*. 2015; 62:849–857.
47. Heffer LF, Fallon JB. A novel stimulus artifact removal technique for high-rate electrical stimulation. *J Neurosci Methods*. 2008;170:277–284.
48. Shivdasani MN, Luu CD, Cicione R, et al. Evaluation of stimulus parameters and electrode geometry for an effective suprachoroidal retinal prosthesis. *J Neural Eng*. 2010;7:036008.
49. Fallon JB, Irvine DRF, Shepherd RK. Cochlear implant use following neonatal deafness influences the cochleotopic organization of the primary auditory cortex in cats. *J Comp Neurol*. 2009;512:101–114.
50. Green DM, Swets JA. *Signal Detection Theory & Psychophysics*. New York: Robert E. Krieger Publishing Co; 1966.
51. Frijns JHM, Dekker DMT, Briaire JJ. Neural excitation patterns induced by phased-array stimulation in the implanted human cochlea. *Acta Otolaryngol*. 2011;131:362–370.
52. Nirenberg S, Pandarinath C. Retinal prosthetic strategy with the capacity to restore normal vision. *Proc Natl Acad Sci U S A*. 2012;109:15012–15017.
53. Abramian M, Lovell NH, Morley JW, Suaning GJ, Dokos S. Activation of retinal ganglion cells following epiretinal electrical stimulation with hexagonally arranged bipolar electrodes. *J Neural Eng*. 2011;8:035004.
54. Gerhardt M, Groeger G, Maccarthy N. Monopolar vs. bipolar subretinal stimulation-an in vitro study. *J Neurosci Methods*. 2011;199:26–34.
55. Kasi H, Bertsch A, Guyomard JL, et al. Simulations to study spatial extent of stimulation and effect of electrode-tissue gap in subretinal implants. *Med Eng Phys*. 2011;33:755–763.
56. Khalili Moghaddam G, Lovell NH, Wilke RGH, Suaning GJ, Dokos S. Performance optimization of current focusing and virtual electrode strategies in retinal implants. *Comput Methods Programs Biomed*. 2014;117:334–342.
57. Warren DJ, Fernandez E, Normann RA. High-resolution two-dimensional spatial mapping of Cat striate cortex using A100-Microelectrode array. *Neuroscience*. 2001;105:19–31.
58. Van den Honert C, Carlyon RP, Long CJ, Smith ZM, Shelton C, Kelsall D. Perceptual evidence of spatially-restricted excitation with focused stimulation. In: Middlebrooks J, Summerfield Q, eds. *CIAP Conference on Implantable Auditory Prostheses, Granlibakken, CA*. University of Southern California; 2007:58.
59. Senn P. *Peripheral nerve stimulation for the treatment of chronic neuropathic pain* [doctoral thesis]. Melbourne, Australia: The University of Melbourne; 2014.
60. Aplin F. *Blind feline model for retinal prosthesis*. [unpublished doctoral thesis]. Melbourne, Australia: The University of Melbourne; September 2015.


Investigative Ophthalmology & Visual Science